Structure of Purine−Purine Mispairs during Misincorporation and Extension by *Escherichia coli* DNA Polymerase I[†]

Angie M. Kretulskie and Thomas E. Spratt*

Department of Biochemistry and Molecular Biology, College of Medicine, The Pennsylvania State University, 500 University Drive, Hershey, Pennsylvania 17033

Received November 10, 2005; Revised Manuscript Received January 13, 2006

ABSTRACT: The mechanism by which purine−purine mispairs are formed and extended was examined with the high-fidelity Klenow fragment of *Escherichia coli* DNA polymerase I with the proofreading exonuclease activity inactivated. The structures of the purine−purine mispairs were examined by comparing the kinetics of mispair formation with adenine versus 7-deazaadenine and guanine versus 7-deazaguanine at four positions in the DNA, the incoming dNTP, the template base, and both positions of the terminal base pair. A decrease in rate associated with a 7-deazapurine substitution would suggest that the nucleotide is in a *syn* conformation in a Hoogsteen base pair with the opposite base. During mispair formation, the k_{pol}/K_d values for the insertion of dATP opposite A (dATP/A) as well as dATP/G and dGTP/G were decreased greater than 10-fold with the deazapurine in the dNTP. These results suggest that during mispair formation the newly forming base pair is in a Hoogsteen geometry with the incoming dNTP in the *syn* conformation and the template base in the *anti* conformation. During mispair extension, the only decrease in k_{pol}/K_d was associated with the G/G base pair in which 7-deazaguanine was in the template strand. These results as well as previous results [McCain et al. (2005) *Biochemistry 44*, 5647−5659] in which a hydrogen bond was found between the 3-position of guanine at the primer terminus and Arg668 during G/A and G/G mispair extension indicate that the conformation of the purine at the primer terminus is in the *anti* conformation during mispair extension. These results suggest that purine−purine mispairs are formed via a Hoogsteen geometry in which the dNTP is in the *syn* conformation and the template is in the *anti* conformation. During extension, however, the conformation of the primer terminus changes to an *anti* configuration while the template base may be in either the *syn* or *anti* conformations.

DNA replication is catalyzed by high-fidelity polymerases that form a mispair once every 10^4-10^6 replication events (*1*). In general, DNA polymerases discriminate against noncomplementary, incorrect nucleotides by binding them more weakly and inserting them more slowly than the complementary, correct dNTP[1] (*2*−*4*). Fidelity is based upon the relative transition state energies during the rate-limiting step (*5*). The rate of mispair formation is only weakly dependent on the identity of the polymerase, indicating that fidelity is dependent on the rate of correct base pair formation (*6*). The similarity in the rate of mispair formation among different polymerases suggests that the mechanisms by which mispairs are formed are similar for all polymerases.

It was originally thought that the correct base was chosen solely on the basis of hydrogen-bonding interactions between the template base and the complementary nucleotide. However, the differences in energy between correctly matched and mismatched bases cannot account for the high fidelity (*7*). Recent investigations have focused on geometric selection as the primary basis of the high fidelity of replication polymerases (*8*−*10*).

It is believed that the purine−pyrimidine mispairs form through wobble conformations and not through the minor tautomers (*2*, *11*−*13*). Purine−purine mispairs can potentially be formed through a variety of mechanisms. Insight into the structures of the mispairs during replication can be obtained from NMR and X-ray crystallography experiments of duplex DNA as well as bound to DNA polymerases.

NMR and X-ray crystal structures of purine−purine mispairs in duplex DNA have found the base pairs to be planar with interstrand hydrogen bonds as illustrated in Charts 1−3. The structures can be categorized on the basis of the conformation of the base relative to the deoxyribose. The mispairs in which both purines are in the *anti* conformation have the Watson−Crick faces interacting (*14*−*18*). The alternative structures have one of the purines in the *syn* conformation and the other in the *anti* conformation (*18*−*24*). In these structures, the *syn*-purine has the Hoogsteen hydrogen-bonding face interacting with the Watson−Crick face of the *anti*-purine. In the *anti*-*syn* structures the 7-position of the *syn*-purine forms a hydrogen bond with the *anti*-purine. The *anti*/*syn* conformations allow the distances

[†] Supported by NIH Grant CA 75074.

* To whom correspondence should be addressed: phone, 717-531-4623; fax, 717-531-7072; e-mail, tes13@psu.edu.

[1] Abbreviations: 7-deaza-dA, 7-deaza-2′-deoxyadenosine; 7-deaza-dG, 7-deaza-2′-deoxyguanosine; BF, *Bacillus stearothermophilis* DNA polymerase large fragment; BSA, bovine serum albumin; dNTP, 2′-deoxyribonucleoside 5′-*O*-triphosphate; DTT, dithiothreitol; EDTA, ethylenediaminetetraacetic acid; KF^+, Klenow fragment of *Escherichia coli* DNA polymerase I; KF^-, Klenow fragment of *E. coli* DNA polymerase I with the proofreading exonuclease inactivated; PAGE, polyacrylamide gel electrophoresis; *Taq*, *Thermus aquaticus*.

10.1021/bi052306u CCC: $33.50
Published on Web 02/22/2006

Chart 1: Structures of A-G Mispairs[a]

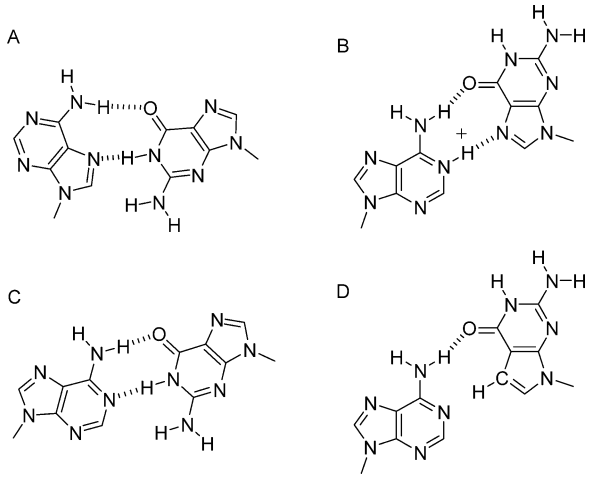

[a] Structures determined by (A) refs *19* and *20*, (B) refs *18* and *20*−*22*, and (C) *14*, *18*, and *25*.

between the C1 positions of the sugars to remain close to the distances observed in B-DNA while the *anti*/*anti* conformation increases the C1 distance by approximately 2 Å.

Crystal structures of purine−purine mispairs were obtained with DNA polymerase I from *Bacillus stearothermophilus* (BF) (*25*), an A-family polymerase, as well as polymerase β (*26*), an X-family polymerase. In these complexes the purine−purine mispair was at the terminal base pair in the postinsertion site, where it would be after the insertion of the mispair and ready to be extended. In the complex with BF, the G/G base pair was found to be in the *syn*/*anti* conformation that is illustrated in Chart 2B (*25*). The A/A base pair was not stable and was observed with the DNA strands frayed. The A/G base pairs were not symmetrical. With A in the primer, the A/G base pair was in the *anti*/*anti* conformation as illustrated in Chart 1C. While with A in the template strand the G/A base pair was frayed. The pol β structure was found to be quite different (*26*). With a terminal A/A base pair and a templating cytosine, the adenine of the template stacks with the primer terminus adenine while the templating cytosine is flipped out of the DNA helix. When dGTP was added, the resulting ternary complex had the templating cytosine within the DNA helix forming Watson−Crick hydrogen bonds with the incoming dGTP. The adenine at the primer terminus was in a *syn* conformation and interacted with the opposite adenine in a planar configuration as illustrated in Chart 3B.

The structures of the polymerases with the mispaired DNA were quite distorted from the structures with Watson−Crick base pairs. It was quite evident that these structures would be unreactive, blocking conformations and not along the reaction pathway for mispair formation or extension. However, these studies can give us clues as to the structure of the DNA and polymerase during mispair formation and extension.

Understanding the mechanism(s) of geometric selection would benefit from knowing the structure of the DNA and polymerase during mispair formation. We have used the hydrogen bond between the 7-position of the *syn*-purine and the Watson−Crick face of the *anti*-purine to discriminate between the possible base pair structure during replication. We have probed the structures of the newly forming base pair as well as the terminal base pair during replication by comparing the kinetics of single base pair incorporation in which 7-deazaadenine and 7-deazaguanine were substituted for adenine and guanine. We have used the Klenow fragment of DNA polymerase I, a highly accurate polymerase for which a wealth of structural, biochemical, and genetic data exist (*27*), as a model to examine the molecular basis of purine−purine mispair formation.

EXPERIMENTAL PROCEDURES

General. [^{32}P]ATP was purchased from NEN at 6000 Ci/mmol. T_4 polynucleotide kinase and the Klenow fragment of *Escherichia coli* DNA polymerase I with the exonuclease activity inactivated (KF^-) were obtained from USB. The dNTPs (ultrapure grade) were purchased from Amersham Biosciences, and the concentrations were determined by UV absorbance (*28*). 2′-Deoxy-7-deazaadenosine (7-deaza-dA) and 2′-deoxy-7-deazaguanosine (7-deaza-dG) were purchased from Berry and Associates (Dexter, MI). The nucleosides were converted into the 5′-triphosphates by the method of Ludlum (*29*). The phosphoramidites for 7-deaza-dA and 7-deaza-dG were purchased from Glen Research. The oligodeoxynucleotides containing 7-deaza-dA and 7-deaza-dG were synthesized, purified by PAGE followed by reverse-phase HPLC, and characterized by mass spectral analysis. The concentrations of oligodeoxynucleotides were determined from the absorbance at 260 nm, using the method of Borer (*30*) in which it was assumed that the spectroscopic properties of 7-deaza-dA and 7-deaza-dG were assumed to be identical to the unmodified nucleotides. The primer was ^{32}P-labeled with [γ-^{32}P]ATP in a reaction catalyzed by T_4 polynucleotide kinase. The oligomer was separated from low molecular weight impurities with a spin column containing Sephadex G-25, and the primer was annealed with a 50% excess of the template as previously described (*31*).

Polymerase Kinetics. The reactions were initiated by the addition of 16 μL of dNTP in 50 mM Tris-HCl (pH 7.8) and 10 mM $MgCl_2$ to 16.4 μL of DNA−enzyme solution in 50 mM Tris-HCl (pH 7.8), 0.1 mM EDTA, 5 mM DTT, and 200 μg/mL BSA at 25 °C with a KinTek-3 rapid quench instrument. The composition of the buffer during the reaction was 50 mM Tris-HCl (pH 7.8), 5 mM $MgCl_2$, 50 μM EDTA, 2.5 mM DTT, and 100 μg/mL BSA. Typically, the DNA concentration was 25 nM, and the polymerase concentration was 100 nM. The reactions were quenched by the addition of 300 mM EDTA. The concentration of dNTPs varied from 0 to 1000 μM. Initial reactions were performed over a wide range of concentrations to determine the approximate K_d values. The experiments used to determine the kinetic parameters that are reported were conducted using concentrations that ranged from 0.2 to 5 times the K_d values. The kinetic parameters reported are from one series of experiments but are consistent with the preliminary experiments and subsequent experiments.

Product Analysis by PAGE. The progress of the reaction was analyzed by denaturing PAGE in 15% acrylamide (19:1 acrylamide:*N*,*N*′-methylenebisacrylamide) and 7 M urea in 1× TBE buffer (0.089 M Tris-HCl, 0.089 M boric acid, 0.002 M Na_2EDTA). The size of the gel was 40 cm × 33 cm × 0.4 mm and was run at 2000 V for 2−2.5 h. The radioactivity on the gel was visualized with a Molecular

Chart 2: Structures of G-G Mispairs[a]

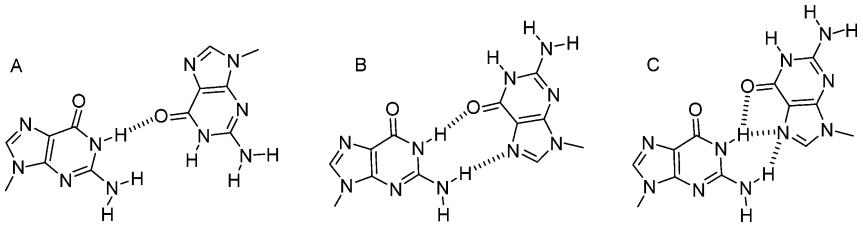

[a] Base pair structures determined by (A) refs *15* and *16*, (B) refs *23*−*25*, and (C) ref *24*.

Chart 3: Structures of A-A Mispairs[a]

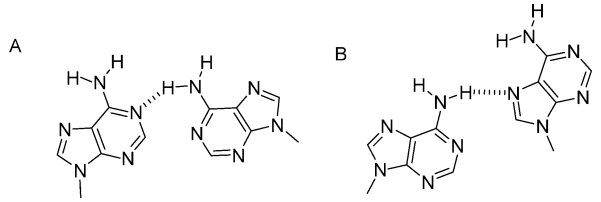

[a] Structure determined (A) in a DNA duplex (*17*) and (B) in the pol β ternary structure (*26*).

Imager FX Pro Plus PhosphorImager. The progress of the reaction was quantitated by dividing the total radioactivity in the product band(s) by the radioactivity in the product and reactant bands. Multiple product bands appeared when the incorrect dNTP was added to the reaction.

Data Analysis. Data were fitted by nonlinear regression using the program Prism version 4 for Windows (GraphPad Software, San Diego, CA, www.graphpad.com). Data from the reactions were fitted to eq 1, where P is the product formed, A is the total amount of DNA reacted, and k is the first-order rate for the dNTP incorporation. The k values for these experiments were fitted to eq 2, where k_{pol} is the maximum rate of dNTP incorporation and K_d is the equilibrium dissociation constant for the interaction of dNTP with the polymerase−DNA complex.

$$P = A(1 - e^{-kt}) \quad (1)$$

$$k = k_{pol}[\text{dNTP}]/([\text{dNTP}] + K_d) \quad (2)$$

RESULTS

7-Deaza-dA and 7-deaza-dG were used as probes for hydrogen bonding between the 7-position of the base and the complementary base during DNA replication. If the nucleotide of interest was in a *syn* conformation, there could be a hydrogen bond between the 7-position of the purine and the complementary base. If this hydrogen bond was important in binding of the dNTP to the polymerase, then the K_d of the deaza-dNTP should increase. If the hydrogen bond was important for phosphodiester bond formation, then the k_{pol} of the reaction would decrease. This approach was recently used to determine that dATP is inserted opposite pyrimidines and thymine dimers in the Watson−Crick and not Hoogsteen or wobble base pairing geometries by DNA polymerase η (*32*). Additionally, it was used to show that DNA polymerase ι uses Hoogsteen base pairing during replication of DNA (*33*).

We measured the time course of incorporation of a single nucleotide into oligodeoxynucleotides using a DNA concentration of 25 nM and a KF concentration of 100 nM. The reactions went to completion, and the time courses followed pseudo-first-order kinetics. The rates of reaction did not increase with 400 nM KF (data not shown), indicating that the polymerase was saturated with DNA and that the reduced rates of reactions observed with mispair formation and extension with and without the 7-deazapurines were not due to decreased binding of the DNA to KF. The single-turnover kinetics were used in favor of steady-state kinetics so that in the analyses of the data we would could ignore the rate of dissociation of the DNA, the step that is rate limiting in replication of DNA (*34*). The first-order rate constants were plotted versus [dNTP], and the k_{pol} and K_d parameters were determined by fitting the data to eq 2. The resulting parameters are presented in Tables 1−4. In general, for the natural nucleotides, the decrease in mispair formation was due to a 200−10000-fold decrease in k_{pol} and a 10−130-fold increase in K_d. Similarly, mispair extension was reduced due to a 1000−30000-fold decrease in k_{pol} and a 10−100-fold increase in K_d.

The 7-deazapurine substitutions did not have much of an effect on the correct base pair formation and extension. The k_{pol}/K_d for the reactions containing 7-deazapurine was within a factor of 2 of that for the natural nucleotides. These results indicate that the nitrogen to carbon substitution does not affect the mechanism of correct base incorporation and extension.

The effect of the 7-deaza-A and 7-deaza-G substitution varied depending on the identity of the mispair and whether it was at the newly forming or the terminal base pair. The relative k_{pol}/K_d values are summarized in Figure 1. In each panel X represents dA, 7-deaza-A, G, or 7-deaza-G, while N represents the base pair partner. The Y axis is the relative k_{pol}/K_d, which is defined as the k_{pol}/K_d of the deazapurine divided by the k_{pol}/K_d of the unmodified purine. The downward bars indicate that the rate of reaction had decreased with the purine to 7-deazapurine substitution.

Panel A shows the results of the experiments in which we tested whether the 7-position of the incoming dNTPs was involved in replication. The correct base pairs, dATP/T and dGTP/C, showed a slight decrease in k_{pol}/K_d due to substitution at the 7-position. This effect was due to an increase in K_d. The rate of incorporation of dATP opposite both A and G was decreased 100- and 10-fold with 7-deaza-dATP, respectively. These reductions in k_{pol}/K_d were due to decreases in k_{pol} as well as increases in K_d. This effect is consistent with the incoming dATP being in the *syn* conformation and forming hydrogen bonds with A and G of the template strand in structures similar to those in Chart 3B and Chart 1A, respectively. The increase in K_d would be due to reduced binding of the 7-deaza-dATP to A or G, perhaps due to the missing hydrogen bond. The decrease in k_{pol} may be due to an altered and suboptimal geometry due

Table 1: 7-Deazapurine Substitution in the Nucleoside Triphosphates[a]

Z[b]	dNTP	k_{pol} (s^{-1})	K_d^{dNTP} (μM)	k_{pol}/K_d^{dNTP} ($s^{-1}\ \mu M^{-1}$)
T	dATP	18.5 ± 0.9	2.2 ± 0.7	8.4 ± 2.7
A	dATP	0.098 ± 0.003	41 ± 6	0.00239 ± 0.0004
G	dATP	0.011 ± 0.001	55 ± 12	0.0002 ± 0.0000
T	d7DATP[c]	23.9 ± 1.2	5.5 ± 2.8	4.3 ± 2.2
A	d7DATP	0.0052 ± 0.0006	284 ± 76	0.000018 ± 0.000005
G	d7DATP	0.003 ± 0.002	167 ± 28	0.000018 ± 0.000012
C	dGTP	13 ± 1.3	2 ± 1	6.5 ± 3.3
A	dGTP	0.0227 ± 0.005	268 ± 179	0.00008 ± 0.00006
G	dGTP	0.0144 ± 0.0007	58 ± 8	0.000248 ± 0.0000
C	d7DGTP[d]	24 ± 8	5 ± 2	4.8 ± 2.5
A	d7DGTP	0.037 ± 0.002	107 ± 14	0.00034 ± 0.00005
G	d7DGTP	0.0025 ± 0.0003	153 ± 81	0.000016 ± 0.000009

[a] Reaction of DNA **1** (Chart 4) with different template bases and dNTPs. The errors for k_{pol} and K_d are the standard errors determined from the nonlinear analysis. The error in k_{pol}/K_d was computed by propagation of errors. [b] Z represents the template base. [c] 2′-Deoxy-7-deazaadenosine 5′-*O*-triphosphate. [d] 2′-Deoxy-7-deazaguanosine 5′-*O*-triphosphate.

Table 2: 7-Deazapurine Substitution at the Template Position[a]

Z[b]	dNTP	k_{pol} (s^{-1})	K_d^{dNTP} (μM)	k_{pol}/K_d^{dNTP} ($s^{-1}\ \mu M^{-1}$)
A	dTTP	96 ± 18	7 ± 3	13.7 ± 6.4
A	dATP	0.062 ± 0.009	79 ± 30	0.00078 ± 0.00032
A	dGTP	0.0098 ± 0.0027	58 ± 25	0.00017 ± 0.00021
7DA[c]	dTTP	165 ± 25	20 ± 10	8.3 ± 4.3
7DA	dATP	0.026 ± 0.006	90 ± 50	0.00029 ± 0.00017
7DA	dGTP	0.012 ± 0.002	56 ± 27	0.00021 ± 0.00011
G	dCTP	68 ± 2	6.4 ± 0.9	10.6 ± 1.5
G	dATP	0.011 ± 0.001	55 ± 13	0.00020 ± 0.00005
G	dGTP	0.026 ± 0.0014	150 ± 45	0.00017 ± 0.00006
7DG[d]	dCTP	38 ± 3	2.0 ± 0.1	19.0 ± 1.6
7DG	dATP	0.038 ± 0.009	124 ± 72	0.00031 ± 0.00019
7DG	dGTP	0.0029 ± 0.0004	35 ± 18	0.00008 ± 0.00004

[a] Reaction of DNA **1** (Chart 4) with different template bases and dNTPs. The errors for k_{pol} and K_d are the standard errors determined from the nonlinear analysis. The error in k_{pol}/K_d was computed by propagation of errors. [b] Z represents the template base. [c] 2′-Deoxy-7-deazaadenosine. [d] 2′-Deoxy-7-deazaguanosine.

Table 3: 7-Deazapurine Substitution at the Primer Terminus[a]

X[b]	Y[b]	k_{pol} (s^{-1})	K_d^{dNTP} (μM)	k_{pol}/K_d^{dNTP} ($s^{-1}\ \mu M^{-1}$)
A	T	17 ± 3	2 ± 1	8.50 ± 4.51
A	A	0.0043 ± 0.0001	92 ± 6	0.000047 ± 0.000003
A	G	0.0045 ± 0.0006	150 ± 50	0.000030 ± 0.000011
7DA[c]	T	17 ± 1	2 ± 1	8.50 ± 4.28
7DA	A	0.00098 ± 0.00016	66 ± 33	0.000015 ± 0.000008
7DA	G	0.0036 ± 0.0008	116 ± 36	0.000031 ± 0.000012
G	C	28.6 ± 2	3.3 ± 1.1	8.67 ± 2.95
G	A	0.001 ± 0.0002	63 ± 10	0.00002 ± 0.00000
G	G	0.004 ± 0.001	130 ± 50	0.00003 ± 0.00001
7DG[d]	C	26.2 ± 0.7	6.4 ± 2.1	4.09 ± 1.35
7DG	A	0.001 ± 0.0002	94 ± 32	0.00001 ± 0.00000
7DG	G	0.007 ± 0.0019	167 ± 40	0.00004 ± 0.00002

[a] Reaction of DNA **2** as shown in Chart 4 with dCTP. The errors for k_{pol} and K_d are the standard errors determined from the nonlinear analysis. The error in k_{pol}/K_d was computed by propagation of errors. [b] X represents the primer terminus and Y its base pair partner. [c] 2′-Deoxy-7-deazaadenosine. [d] 2′-Deoxy-7-deazaguanosine.

to the fact that the 7-deaza-dATP cannot fit snuggly against A or G.

The misincorporation of dGTP opposite G showed similar results. The k_{pol}/K_d for the incorporation of 7-deaza-dGTP opposite G was decreased 15-fold relative to dGTP. Again, the decrease in k_{pol}/K_d was due to a decrease in k_{pol} and an increase in K_d. This result is consistent with dGTP adopting a *syn* conformation to form the Hoogsteen base pair with the template G as illustrated in Chart 2B or Chart 2C.

The effect of the substitutions for the incorporation of dGTP opposite A showed different results. The 7-deaza-dGTP substitution in the opposite A was increased only slightly (4-fold). This result is suggestive that dGTP is in the *anti* conformation. However, the lack of an effect on the deaza substitution is not indisputable proof that the nucleotide is in the *anti* conformation. It is possible that the N7-position may be involved in a hydrogen bond but that elimination of the hydrogen bond does not result in a decrease in rate. For example, the potential dGTP(*syn*)/A(*anti*) structure in Chart 1B is protonated. Substitution of the N at the 7-position with CH would involve loss of a hydrogen bond. However, the stability that the hydrogen bond provided may be offset by the loss of the positive charge. 7-Deaza-dGTP may be inserted opposite A by the structure illustrated in Chart 1D,

Table 4: 7-Deazapurine Substitution at the Template Strand in the Terminal Base Pair[a]

X[b]	Y[b]	k_{pol} (s^{-1})	K_d^{dNTP} (μM)	k_{pol}/K_d^{dNTP} (s^{-1} μM^{-1})
T	A	37 ± 1	3 ± 1	12.3 ± 4.1
A	A	0.0065 ± 0.0008	108 ± 31	0.00006 ± 0.00002
G	A	0.0094 ± 0.0013	36 ± 17	0.00026 ± 0.00013
T	7DA[c]	21 ± 1	1.9 ± 0.3	11.1 ± 1.8
A	7DA	0.0028 ± 0.0005	70 ± 26	0.00004 ± 0.00002
G	7DA	0.012 ± 0.001	37 ± 9	0.00031 ± 0.00008
C	G	59 ± 2	4 ± 0.4	14.8 ± 1.6
A	G	0.0081 ± 0.0007	69 ± 14	0.00012 ± 0.00003
G	G	0.0489 ± 0.0054	55 ± 16	0.00089 ± 0.00028
C	7DG[d]	61.8 ± 0.3	4.8 ± 0.2	12.9 ± 0.5
A	7DG	0.0068 ± 0.0009	22.3 ± 12.3	0.00030 ± 0.00017
G	7DG	0.00080 ± 0.00018	25 ± 9	0.000032 ± 0.000014

[a] Reaction with DNA **3** (Chart 4) and dATP. The errors for k_{pol} and K_d are the standard errors determined from the nonlinear analysis. The error in k_{pol}/K_d was computed by propagation of errors. [b] X represents the primer terminus and Y its base pair partner. [c] 2′-Deoxy-7-deazaadenosine. [d] 2′-Deoxy-7-deazaguanosine.

Chart 4: Sequences of Oligodeoxynucleotide Duplexes Used in This Study

```
5′- G C A C C G C A G A C G C A G          -3′   1
3′- C G T G G C G T C T G C G T C Z T C A G C G T C  -5′

5′- G C A C C G C A G A C G C A X          -3′   2
3′- C G T G G C G T C T G C G T Y G T C A G C G T C  -5′

5′- G C A C C G C A G A C G C A G X        -3′   3
3′- C G T G G C G T C T G C G T C Y T C A G C G T C  -5′
```

very similar to the structure of dGTP/G as illustrated in Chart 1B. There is evidence of the instability of the dGTP(*syn*)/A(*anti*) structure in the kinetic parameters. The K_d for dGTP in the incorporation opposite A is 268 μM. This value is approximately 5-fold larger than the three other purine−purine misincorporation K_ds in this study. The k_{pol}/K_d for the incorporation of dGTP opposite A is almost as slow as that for the deaza-substituted reactions.

We examined the conformation of the template base with the 7-deazapurine substitutions. Panel B shows that the substitutions had no effect on k_{pol}/K_d. These results indicate that the 7-position of the purines was not involved in a critical hydrogen bond during replication. The results for dATP/A, dATP/G, and dGTP/G complement the results in panel A, in that the results are consistent with the dNTP being in the *syn* conformation and the template being in the *anti* conformation. The results for dGTP/A show no effect for the deaza substitutions and as described above are inconclusive as to the structure of the base pair.

We examined the conformations of the base pairs in the terminal base pair with the 7-deazapurine substitutions. Panel C shows that the substitutions in the primer strand had no effect on k_{pol}/K_d. Panel D shows that the G to 7-deaza-G substitution in the template strand with G in the primer strand resulted in a 26-fold reduction in k_{pol}/K_d that was primarily due to a decrease in k_{pol}. The reduction in rate for 7-deaza-dG in the template strand indicates that this nucleotide is in the *syn* conformation with the N7-position in a hydrogen bond with the G on the primer strand. The lack of an effect for the dG to 7-deaza-dG substitution on the primer terminus suggests that this nucleotide is in the *anti* conformation. Thus both the primer and template results are consistent with the G/G base pair to be in the *anti*/*syn* conformation. The lack of an effect for the deaza substitutions for both the primer and template strands for the A/A, A/G, and G/A base pairs suggests that these base pairs are in the *anti*/*anti* conformations. This assignment is not without qualification, however. It is possible for one of the base pairs to be in the *syn*/*anti* conformation but with the proviso that the hydrogen bond between the N7-position of the *syn*-purine with the *anti*-purine is not important in binding of the dNTP or in the polymerization steps.

DISCUSSION

Replication proceeds by threading the DNA through the polymerase. For A-family polymerases, the template base is initially in the preinsertion site in the *syn* conformation. As it moves from the preinsertion site to the insertion site, it rearranges to the *anti* conformation and pairs with an incoming base. After phosphodiester bond formation takes place, the newly synthesized base moves into the postinsertion site (*35*). Polymerases are efficient at preventing mismatches from occurring by reducing the efficiency of mispair formation and then subsequently reducing the rate of mismatch extension (*36*). The reduced rate of extension allows the exonuclease activity that many of the polymerases contain to excise incorrectly incorporated base. Crystal structures of BF and pol β with mispairs at the terminal base pair illustrate possible blocking conformations (*25*, *26*). The insertion or extension of a mispair is a rare event, and trapping of the active mispair conformation might be difficult. We have used kinetic studies to probe these configurations.

Our results indicate that for the dATP/A, dATP/G, and dGTP/G base pairs in the insertion site, the dNTPs are in the *syn* conformation while the template bases are in the *anti* conformation. The results for the incorporation of dGTP/A were suggestive of an *anti*/*anti* conformation but do not absolutely exclude having the incoming dGTP in the *syn* conformation. The *syn*/*anti* conformation of the dNTP/template base pair would allow the distances between the 1-positions of the respective deoxyribose groups to maintain a Watson−Crick B-DNA distance. This distance may be critical for aligning the triphosphate with the 3′-terminal hydroxyl group. The *anti*/*anti* conformation would increase the distance between the 1-positions of the deoxyribose moieties by 1.5−2 Å.

Our results for the structure of the terminal base pair are not as conclusive. The results for the G/G base pair indicate that the primer strand G is in the *anti* conformation while the template G is in the *syn* conformation. This result would

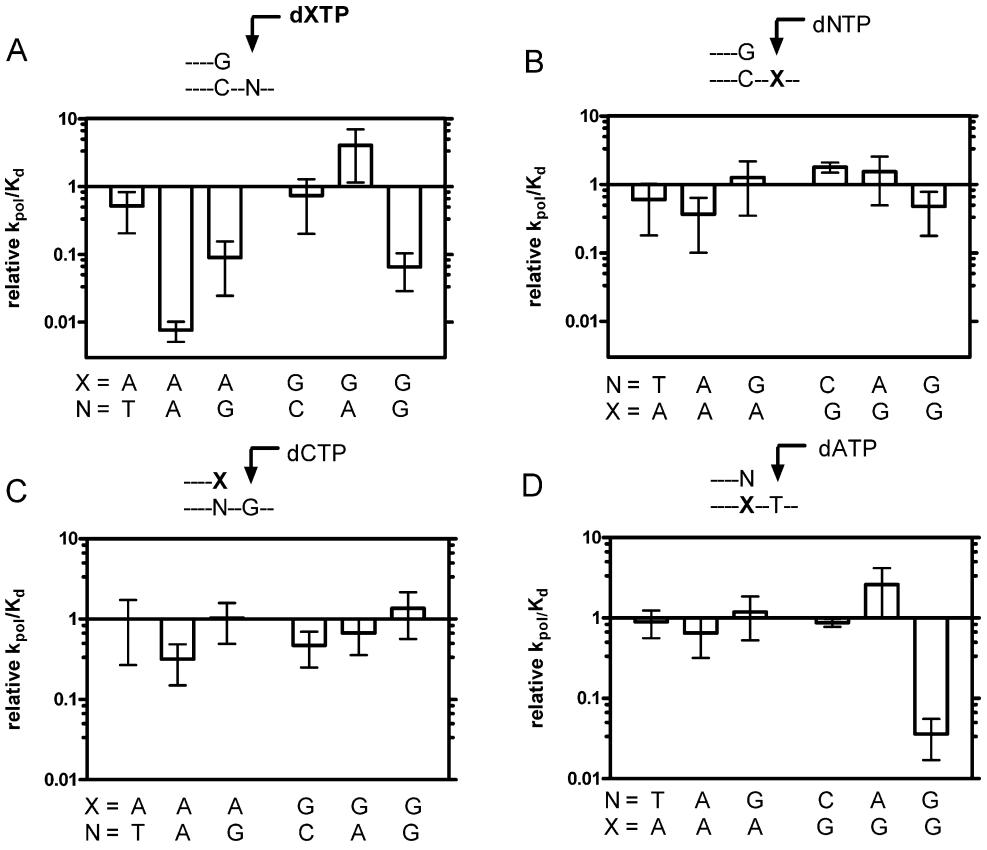

FIGURE 1: Relative k_{pol}/K_d for single-nucleotide incorporation for the substitution of 7-deazaadenine for adenine and 7-deazaguanine for guanine at (A) the incoming dNTP, (B) the template base, (C) the primer terminus, and (D) the template position of the terminal base pair. The *Y* axis is the $(k_{pol}/K_d)^{deazapurine}/(k_{pol}/K_d)^{purine}$. X = A represents the 7-deaza-dA/A substitution, and X = G represents the 7-deaza-dG/G substitution. N is the base pair partner to X. The effort bars were computed by propagation of errors.

Scheme 1: Kinetic Scheme for DNA Replication

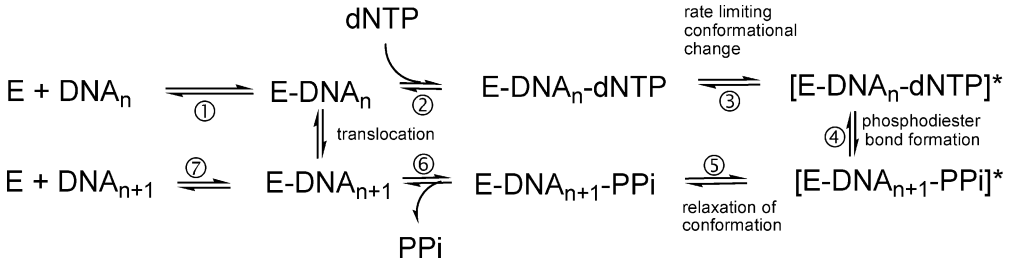

indicate that the *syn*/*anti* conformation of the insertion site must be reversed to an *anti*/*syn* conformation in the postinsertion site in order for the G/G mispair to be extended. This result is consistent with results we obtained previously when we examined the interaction between Arg668 and the primer terminus G using 3-deaza-dG. In those experiments we concluded that there was a hydrogen bond between Arg668 and the N3-position of G at the primer terminus for the extension of G/A and G/G mispairs (*37*). This hydrogen bond could only occur if the G at the primer terminus was in the *anti* conformation. In the KF, a major mechanism by which the fidelity of formation and extension is enhanced is by a hydrogen-bonding fork between Arg668 and the minor groove of the primer terminus as well as the ring oxygen of the incoming dNTP (*37*−*44*). Elimination of this interaction causes a decrease in the fidelity of this polymerase (*37*, *44*). This interaction may be the reason the incoming dNTP rearranges from the *syn* to *anti* conformation with purine−purine mispairs.

The arginine fork between the incoming dNTP and primer terminus is a feature of A-family polymerases that is not present in other polymerases. If the hydrogen bond between Arg668 and the minor groove of the primer terminus is the reason for the shift from *syn* to *anti* conformation, it might not occur in other polymerases. Another factor that could affect the geometry of the base pairs is the sequence context.

ACKNOWLEDGMENT

The molecular imaging of the polyacrylamide gels and the synthesis of the oligodeoxynucleotides used in this study were carried out in the Macromolecular Core Facility of The Pennsylvania State University College of Medicine.

REFERENCES

1. Kunkel, T. A. (2004) *J. Biol. Chem. 279*, 16895−16898.
2. Goodman, M. F., Creighton, S., Bloom, L. B., and Petruska, J. (1993) *Crit. Rev. Biochem. Mol. Biol. 28*, 83−126.
3. Goodman, M. F. (1988) *Mutat. Res. 200*, 11−20.

4. Johnson, K. A. (1993) *Annu. Rev. Biochem. 62*, 685−713.
5. Showalter, A. K., and Tsai, M. D. (2002) *Biochemistry 41*, 10571−10576.
6. Beard, W. A., Shock, D. D., Vande Berg, B. J., and Wilson, S. H. (2002) *J. Biol. Chem. 277*, 47393−47398.
7. Petruska, J., Goodman, M. F., Boosalis, M. S., Sowers, L. C., Cheong, C., and Tinoco, I., Jr. (1988) *Proc. Natl. Acad. Sci. U.S.A. 85*, 6252−6256.
8. Sloane, D. L., Goodman, M. F., and Echols, H. (1988) *Nucleic Acids Res. 16*, 6465−6475.
9. Echols, H., and Goodman, M. F. (1991) *Annu. Rev. Biochem. 60*, 477−511.
10. Kool, E. T. (2002) *Annu. Rev. Biochem. 71*, 191−219.
11. Brown, T., Hunter, W. N., Kneale, G., and Kennard, O. (1986) *Proc. Natl. Acad. Sci. U.S.A. 83*, 2402−2406.
12. Joyce, C. M., Sun, X. C., and Grindley, N. D. (1992) *J. Biol. Chem. 267*, 24485−24500.
13. Minnick, D. T., Liu, L., Grindley, N. D. F., Kunkel, T. A., and Joyce, C. M. (2002) *Proc. Natl. Acad. Sci. U.S.A. 99*, 1194−1199.
14. Prive, G. G., Heinemann, U., Chandrasegaran, S., Kan, L. S., Kopka, M. L., and Dickerson, R. E. (1987) *Science 238*, 498−504.
15. Borden, K. L., Jenkins, T. C., Skelly, J. V., Brown, T., and Lane, A. N. (1992) *Biochemistry 31*, 5411−5422.
16. Faibis, V., Cognet, J. A., Boulard, Y., Sowers, L. C., and Fazakerley, G. V. (1996) *Biochemistry 35*, 14452−14464.
17. Gervais, V., Cognet, J. A., Le Bret, M., Sowers, L. C., and Fazakerley, G. V. (1995) *Eur. J. Biochem. 228*, 279−290.
18. Gao, X., and Patel, D. J. (1988) *J. Am. Chem. Soc. 110*, 5178−5182.
19. Hunter, W. N., Brown, T., and Kennard, O. (1986) *J. Biomol. Struct. Dyn. 4*, 173−191.
20. Brown, T., Leonard, G. A., Booth, E. D., and Chambers, J. (1989) *J. Mol. Biol. 207*, 455−457.
21. Leonard, G. A., Booth, E. D., and Brown, T. (1990) *Nucleic Acids Res. 18*, 5617−5623.
22. Lane, A. N., Jenkins, T. C., Brown, D. J., and Brown, T. (1991) *Biochem. J. 279* (Part 1), 269−281.
23. Cognet, J. A., Gabarro-Arpa, J., Le Bret, M., van der marel, G. A., van Boom, J. H., and Fazakerley, G. V. (1991) *Nucleic Acids Res. 19*, 6771−6779.
24. Skelly, J. V., Edwards, K. J., Jenkins, T. C., and Neidle, S. (1993) *Proc. Natl. Acad. Sci. U.S.A. 90*, 804−808.
25. Johnson, S. J., and Beese, L. S. (2004) *Cell 116*, 803−816.
26. Batra, V. K., Beard, W. A., Shock, D. D., Pedersen, L. C., and Wilson, S. H. (2005) *Structure (Cambridge) 13*, 1225−1233.
27. Joyce, C. M., and Steitz, T. A. (1994) *Annu. Rev. Biochem. 63*, 777−822.
28. Dunn, D. B., and Hall, R. H. (1986) in *Handbook of Biochemistry and Molecular Biology* (Fasman, G. D., Ed.) pp 65−215, CRC Press, Boca Raton, FL.
29. Ludwig, J. (1981) *Acta Biochim. Biophys. Acad. Sci. Hung. 16*, 131−133.
30. Borer, P. (1977) in *Handbook of Biochemistry and Molecular Biology* (Fasman, G. D., Ed.) p 589, CRC Press, Boca Raton, FL.
31. Spratt, T. E., and Campbell, C. R. (1994) *Biochemistry 33*, 11364−11371.
32. Hwang, H., and Taylor, J. S. (2005) *Biochemistry 44*, 4850−4860.
33. Johnson, R. E., Prakash, L., and Prakash, S. (2005) *Proc. Natl. Acad. Sci. U.S.A. 102*, 10466−10471.
34. Kuchta, R. D., Mizrahi, V., Benkovic, P. A., Johnson, K. A., and Benkovic, S. J. (1987) *Biochemistry 26*, 8410−8417.
35. Kiefer, J. R., Mao, C., Braman, J. C., and Beese, L. S. (1998) *Nature 391*, 304−307.
36. Joyce, C. M., and Benkovic, S. J. (2004) *Biochemistry 43*, 14317−14324.
37. McCain, M. D., Meyer, A. S., Glekas, A., and Spratt, T. E. (2005) *Biochemistry 44*, 5647−5659.
38. Morales, J. C., and Kool, E. T. (1999) *J. Am. Chem Soc. 121*, 2323−2324.
39. Morales, J. C., and Kool, E. T. (2000) *Biochemistry 39*, 12979−12988.
40. Doublie, S., Tabor, S., Long, A. M., Richardson, C. C., and Ellenberger, T. (1998) *Nature 391*, 251−258.
41. Li, Y., Korolev, S., and Waksman, G. (1998) *EMBO J. 17*, 7514−7525.
42. Spratt, T. E. (2001) *Biochemistry 40*, 2647−2652.
43. Meyer, A. S., Blandino, M., and Spratt, T. E. (2004) *J. Biol. Chem. 279*, 33043−33046.
44. Minnick, D. T., Bebenek, K., Osheroff, W. P., Turner, R. M., Jr., Astatke, M., Liu, L., Kunkel, T. A., and Joyce, C. M. (1999) *J. Biol. Chem. 274*, 3067−3075.

BI052306U